Journal of Dental Sciences 20 (2025) 1723–1730

Available online at www.sciencedirect.com

ScienceDirect

journal homepage: www.e-jds.com

Original Article

Evaluation of the physical and mechanical properties of 3D-printed resin for orthodontic fixed lingual retainers: An *in vitro* study

Pyi Phyo Win [a,b], Szu-Yu Lai [a], Daniel De-Shing Chen [a,b], Bolormaa Sainbayar [c], Tzu-Yu Peng [a*], Johnson Hsin-Chung Cheng [a,b**]

[a] *School of Dentistry, College of Oral Medicine, Taipei Medical University, Taipei, Taiwan*
[b] *Division of Orthodontics, Department of Dentistry, Taipei Medical University Hospital, Taipei, Taiwan*
[c] *School of Dentistry, Mongolian National University of Medical Sciences, Ulaanbaatar City, Mongolia*

Received 16 March 2025; Final revision received 26 March 2025
Available online 10 April 2025

KEYWORDS
3D-printed resin;
Orthodontics;
Fixed lingual retainer;
Water sorption and solubility;
Staining;
Flexural performance

Abstract *Background/Purpose:* Fixed lingual retainers (FLRs) often experience structural instability, including poor adaptation, and the untwisting of spiral wires, which can lead to unwanted tooth movement. Digital workflows have enhanced the appliance's accuracy. This study evaluated the water sorption (W_{sp}), water solubility (W_{sl}), staining resistance, and flexural performance of three-dimensionally printed resin (3DR) to determine its optimal design for FLRs.

Materials and methods: Cylindrical 3DR specimens were immersed in distilled water and artificial saliva for 7, 14, and 30 days. W_{sp} and W_{sl} were measured according to ISO 4049 guidelines. Color stability was analyzed after 7 days of immersion in staining solutions using the CIEDE2000 formula. Straight 3DR specimens with various cross-sectional shapes and dimensions underwent a three-point bending test, comparing mechanical properties to multistrand stainless-steel wire (MSW). Statistical analysis was performed using a one-way ANOVA with Tukey's post-hoc test ($P < 0.05$).

Results: W_{sp} and W_{sl} values remained within ISO standards, with no significant changes over time. Specimens exposed to red wine, grape juice, and curry exhibited color changes exceeding the acceptability threshold of 1.77, while other solutions caused minimal discoloration. Hemi-elliptical cross-sections demonstrated significantly greater flexural strength than

* Corresponding author. School of Dentistry, College of Oral Medicine, Taipei Medical University, 250 Wu-Hsing Street, Taipei 11031, Taiwan.
** Corresponding author. School of Dentistry, College of Oral Medicine, Taipei Medical University, 250 Wu-Hsing Street, Taipei 11031, Taiwan.
E-mail addresses: typeng@tmu.edu.tw (T.-Y. Peng), g4808@tmu.edu.tw (J. Hsin-Chung Cheng).

https://doi.org/10.1016/j.jds.2025.03.034

round designs. Although all 3DR specimens fractured before reaching the 2.0-mm deflection limit, some designs exhibited comparable bending strength to MSW while maintaining sufficient flexibility for physiological tooth movement.
Conclusion: A hemi-elliptical 3DR design (1.0 mm thick and 2.0 mm wide) demonstrated stability in the oral environment, moderate stainability, and mechanical performance comparable to MSW, supporting its feasibility for FLRs.

Introduction

Retainers are essential for maintaining post-orthodontic alignment and preventing relapse.[1] While both fixed and removable retainers are used in practice, studies indicated that patients struggle with consistent use of removable retainers.[2,3] Materials and designs of fixed lingual retainers (FLRs), introduced by Knierim in 1973,[4] have since evolved.[5,6] Multistrand stainless-steel wires (MSWs) are widely used, but fiber-reinforced composites (FRCs) offer aesthetic and biocompatibility advantages,[7,8] with studies showing reduced incidence of relapse compared to MSWs.[9] A study conducted by Andrea found that based on a visual analog scale, patients reported greater satisfaction with tooth-colored bonded retainers compared to MSWs.[10]

One of the key criteria for FLRs is precise adaptation to the tooth surface to prevent undesirable tooth movement.[11,12] Advances in computer-aided design and manufacturing (CAD/CAM) enable more accurate and passive adaptation. As a result, research has expanded exploration of metal-free alternatives such as zirconia, FRCs, and polyetheretherketone.[13–15] FLRs can be fabricated using subtractive milling and additive three-dimensional (3D) printing. While milling provides high strength and durability, it results in significant material waste and frequent wear on the burs.[16] Conversely, 3D printing offers faster, cost-effective production with less material waste, although concerns remain regarding polymerization shrinkage and surface roughness.[17] Several studies examined different 3D printing materials for their potential use in FLRs.[18,19] However, gaps remain in understanding their dimensional and color stability, as well as their optimal design for clinical use. In this study, we evaluated the physical and optical stability of 3D printed resin (3DR) and determined the most effective design for use as an FLR.

Materials and methods

Sample size calculation

In total, five specimens ($n = 5$) per group were allocated for the water sorption (W_{sp}) and water solubility (W_{sl}) tests, following ISO 4049 procedures.[20] Based on Abdullah et al.,[15] the sample size was calculated using an 80 % statistical power ($\beta = 0.2$) and a 5 % significance level ($\alpha = 0.05$) to detect a primary outcome of 0.555 for both a color difference (ΔE_{00}) and a three-point bending test (TPBT). The minimum required sample size was determined to be seven specimens ($n = 7$) per group for these experiments. Calculations were performed using G*Power vers. 3.1.9.6 (Heinrich Heine University, Düsseldorf, Germany).

Specimen preparation

Cylindrical 3DR specimens (Detax freeprint crown, Detax GmbH & Co. KG, Ettlingen, Germany), measuring 10 mm in diameter and 2.5 mm in thickness were designed and printed using a 3D printing machine (3Demax, DMG Medical Devices, Hamburg, Germany). In total, 86 specimens were fabricated, comprising 30 specimens for the W_{sp} and W_{sl} tests ($n = 30$) and 56 specimens for the ΔE_{00} test ($n = 56$). Specimens were polished with 600-grit abrasive paper until a smooth surface with a uniform color was achieved.

Thirty-five straight specimens, each measuring 30 mm in length, were prepared for the TPBT. Detailed dimensions, cross-sectional shapes and the groups' name abbreviations are provided in Table 1. Specimens were also designed and printed out as shown in Fig. 1. Additionally, conventional 0.5 mm (~0.0195 inches) MSW (G&H Orthodontics, Franklin, IN, USA) served as a control. Specimens were divided into six groups, each consisting of seven specimens ($n = 42$).

Water sorption (W_{sp}) and solubility (W_{sl}) measurements
Among 30 cylindrical specimens, 15 were immersed in distilled water (DW) and 15 in artificial saliva (AS; BZ 109, Biochemazone, Alberta, Canada). Each group was further subdivided into three subgroups of five specimens each, based on the immersion duration: 7 days (7D), 14 days (14D), and 30 days (30D).

Table 1 Dimensions, cross-sectional shapes, and abbreviations of 3D-printed resin specimens for the three-point bending test.

Groups	Dimensions
Round (R)	Diameter (mm)
R1.5	1.5
R2.0	2.0
Hemi-elliptical (H)	Thickness × Width (mm)
H1.0	1.0 × 2.0
H1.5	1.5 × 3.0
H2.0	2.0 × 4.0

Thickness refers to the faciolingual dimension, while width refers to the inciso-cervical dimension.

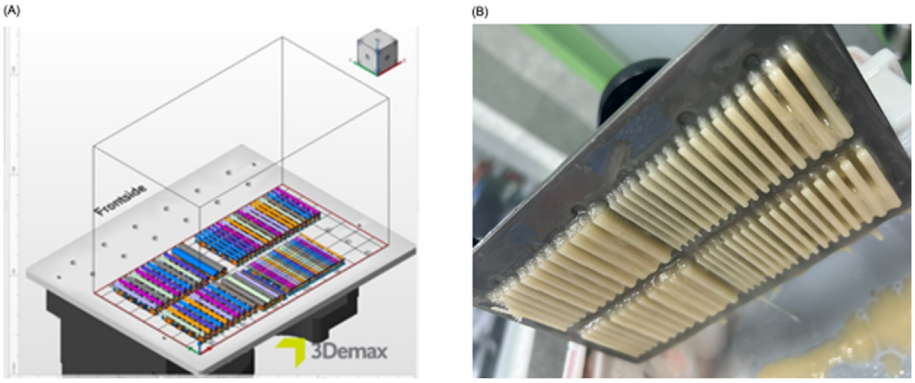

Figure 1 Production of 3D-printed resin (3DR) specimens for the three-point bending test (A) digital layout of 3D models on the build plate and (B) 3DR specimens immediately after printing.

Specimens were conditioned in an oven at 37 ± 2 °C for 22 h, followed by storage at room temperature with silica gel for 2 h. The mass of each specimen was measured using a precision balance, and this cycle was repeated until a constant mass (m_1) was achieved, with variations of <1.0 μg over a 24-h interval. Once a stable mass was obtained, the diameter of each sample was measured at two points perpendicular to each other, and the mean value was recorded. The thickness was then measured at the center of each specimen at two locations using a digital caliper, and the mean was calculated. Finally, the volume was determined.

Specimens were subsequently submerged in individual culture wells containing their respective solutions (DW and AS) and labeled according to the immersion period (7D, 14D and 30D). They were stored in the oven at 37 ± 2 °C. At the end of each designated period, specimens were removed from the solution, gently dried on filter paper until free from visible moisture and weighed 1 min after removal to obtain the mass (m_2). Following this, specimens were reconditioned using the same initial procedure until a constant dry mass (m_3) was achieved. The diameter and thickness of each specimen were measured at the same locations and recorded after weighing for both m_2 and m_3.

W_{sp} and W_{sl} were calculated using formulas defined by ISO 4049:

$$W_{sp} = \frac{m_2 - m_3}{V} \text{ and} \quad (1)$$

$$W_{sl} = \frac{m_1 - m_3}{V}; \quad (2)$$

where m_1 is the initial mass, m_2 is the mass after immersion, m_3 is the final dry mass, and V is the volume of the specimen. The material was considered suitable for intraoral use with minimal water absorption concerns if the value was less than or equal to 40 μg/mm^3 and suitable for use without significant chemical diffusion if the value was less than or equal to 7.5 μg/mm^3.

Color difference (ΔE_{00}) measurement

The surface roughness (Ra) of all 56 specimens was measured using a profilometer (Surftest SJ-210, Mitutoyo, Tokyo, Japan) with a total measurement length of 6.4 mm, a cutoff length of 0.8 mm, and a measuring speed of 0.5 mm/s. Three readings were taken for each specimen, and the average roughness value was calculated. Specimens were polished or reprinted until the roughness value ranged 0.82–0.98 μm.

The pH of test solutions was measured three times with a calibrated pH meter (FiveEasy Plus pH meter FP20, Mettler Toledo, Greifensee, Switzerland) to assess its potential effect on staining.[21]

Color (T_1) was measured using a digital colorimeter (OptiShade Styleitaliano, Smile Line, St-Imier, Switzerland). The spectrophotometer was calibrated following the device's instructions, and the CIELAB parameters (L*, a*, b*) of each specimen were recorded against a gray calibration card (QP Card 101, QPcard AB, Helsingborg, Sweden). After the initial color measurements, specimens were divided into eight groups, each containing seven samples: a control DW, AS, black coffee (BC), cola, black tea (BT), curry (CR), grape juice (GJ), and red wine (RW). Specimens were stored at room temperature for 7D.[22] Solutions were renewed every 2 days to prevent bacterial and fungal contamination. After 7D of staining, samples were thoroughly clean in DW and gently dried on filter paper until free from visible moisture. Samples were then remeasured (T_2). The ΔE_{00} between T_1 and T_2 was calculated using the following CIEDE2000 formula:[23]

$$\Delta E_{00} = \sqrt{\left(\frac{\Delta L'}{k_L S_L}\right)^2 + \left(\left(\frac{\Delta C'}{k_c S_C}\right)^2 + \left(\left(\frac{\Delta H'}{k_H S_H}\right)^2 + R_T \left(\left(\frac{\Delta C'}{k_C S_C}\right)\left(\left(\frac{\Delta H'}{k_H S_H}\right)\right.\right.\right.} \quad (3)$$

where $\Delta L'$, $\Delta C'$, and $\Delta H'$ respectively represent differences in lightness, chroma, and hue. The terms k_L, k_C, and k_H denote weighting factor for lightness, chroma, and hue, while S_L, S_C, and S_H correspond to mean coefficients for each attribute. The term R_T indicates an overall calibration coefficient based on combined differences in chroma and hue.

Color differences were assessed using the thresholds for 50 %:50 % color perceptibility (PT_{00}) of 0.81 and color acceptability (AT_{00}) of 1.77.[24]

Three-point bending test (TPBT)

The TPBT was conducted using a universal testing machine (JSV-H1000, Japan Instrumentation System, Nara, Japan) following ISO 15841.[25] Specimens were supported 10.0 mm from each edge, a crosshead speed of 1.0 mm/min was applied at the center, and loading continued until a crosshead displacement of 2.0 mm was reached. Forces corresponding to each 0.1-mm deflection, up to 2.0 mm, were recorded during testing. The flexural strength for each cross-sectional shape and dimension was calculated using the following equations and were compared across 3DR specimens:[26]

$$\sigma_R = \frac{8FL}{\pi d^3} \text{ and} \quad (4)$$

$$\sigma_H = \frac{2FL}{\pi ab^2}; \quad (5)$$

where σ_R denotes the flexural strength of a round wire, F is the applied load, L is the span length, and r is the radius of the round wire. For a hemi-elliptical wire, σ_H represents the flexural strength, and a and b are the semi-major and semi-minor axes, respectively.

Additionally, the performance of the 3DR was analyzed through the load-deflection curve and compared to that of the control MSW. Based on the results, the optimal shape and dimensions of the 3DR for use as an FLR were selected.

Statistical analysis

Data were analyzed using standard statistical software (IBM SPSS version 19.0, Armonk, NY, USA) with a significance level set to 5 % ($P < 0.05$). A one-way analysis of variance (ANOVA) with Tukey's post-hoc test was used to compare W_{sp} and W_{sl} between DW and AS and across immersion durations (7D, 14D, and 30D). Additionally, the same analysis was employed to evaluate ΔE_{00} among solutions after 7D of immersion, flexural strength across 3DR specimens with various designs, and the maximum deflection under load among 3DR specimens, including MSW.

Results

Water sorption (W_{sp}) and solubility (W_{sl}) measurements

Specimens were immersed in DW and AS for 7, 14, and 30 days. In DW, mean sorption values were 5.67 ± 0.19 μg/mm^3 (7D), 7.77 ± 4.88 μg/mm^3 (14D), and 8.08 ± 2.89 μg/mm^3 (30D). In AS, mean values were 4.63 ± 2.63 μg/mm^3 (7D), 5.63 ± 0.34 μg/mm^3 (14D), and 3.49 ± 3.19 μg/mm^3 (30D). The one-way ANOVA with Tukey's test showed no significant differences across time points within each solution (Fig. 2A). For the solubility test, mean values in DW were −3.44 ± 3.14 μg/mm^3 (7D), −4.35 ± 4.67 μg/mm^3 (14D), and −5.84 ± 0.37 μg/mm^3 (30D). In AS, mean values were −4.63 ± 2.63 μg/mm^3 (7D), −4.47 ± 2.52 μg/mm^3 (14D), and −6.98 ± 2.20 μg/mm^3 (30D). No significant differences were observed across time points within each solution (Fig. 2B). Comparisons between DW and AS at corresponding time points also revealed no significant differences (Fig. 2A and B). All W_{sp} and W_{sl} values remained within ISO 4049 limits (40 μg/mm^3 for W_{sp} and 7.5 μg/mm^3 for W_{sl}). No significant changes in the diameter, thickness, or volume were detected after immersion (Table 2).

Color difference (ΔE_{00}) measurement

The pH levels of the solutions were recorded as follows: DW (9.44 ± 0.06), AS (7.40 ± 0.07), BC (5.42 ± 0.09), cola (2.48 ± 0.02), BT (6.17 ± 0.15), CR (5.60 ± 0.03), GJ (3.73 ± 0.05), and RW (3.41 ± 0.06). Specimens were immersed in the solutions for 7D, and mean ΔE_{00} values are illustrated in Fig. 3. Color measurements were taken before and after staining, with readings conducted against a gray background to minimize color distortion and ensure more-accurate color perception.[27] The ΔE_{00} value of the RW group showed a significant change compared to the other groups with a mean value of 13.33 ± 1.06. The GJ and CR groups followed, with respective mean values of 2.57 ± 0.40 and 2.40 ± 0.45, and no significant difference between them. However, ΔE_{00} values of these three groups exceeded the acceptability threshold of 1.77. Additionally, the BC, BT, and AS groups exhibited mean ΔE_{00} values above the perceptible color difference threshold of 0.81, with respective values of 1.47 ± 0.24, 1.12 ± 0.38, and 0.95 ± 0.07, although no significant differences were observed between these groups. Interestingly, the cola group had a ΔE_{00} value of 0.42 ± 0.11, showing no significant difference compared to the DW group (0.47 ± 0.06) or the AS group. The coke and DW groups remained below the perceptibility limits.

Three-point bending test (TPBT)

The TPBT evaluated the flexural strength, maximum bending force, and deflection. The flexural strength of round wires was significantly lower than that of hemi-elliptical wires (Table 3). Among the round wire groups, R1.5 exhibited a flexural strength of 25.33 ± 3.33 MPa, while R2 registered 22.92 ± 3.26 MPa, with no statistically significant difference between them. In contrast, within the hemi-elliptical wire group, H1 achieved the highest flexural strength, with a maximum stress value of 218.47 ± 57.54 MPa, despite its smaller dimensions. H1 also demonstrated a statistically significant difference in flexural strength compared to the other specimens. No significant difference was observed between H1.5 (152.43 ± 58.77 MPa) and H2.0 (150.91 ± 32.20 MPa). Based on its flexural strength, H1 exhibited superior stress resistance compared to the other specimens.

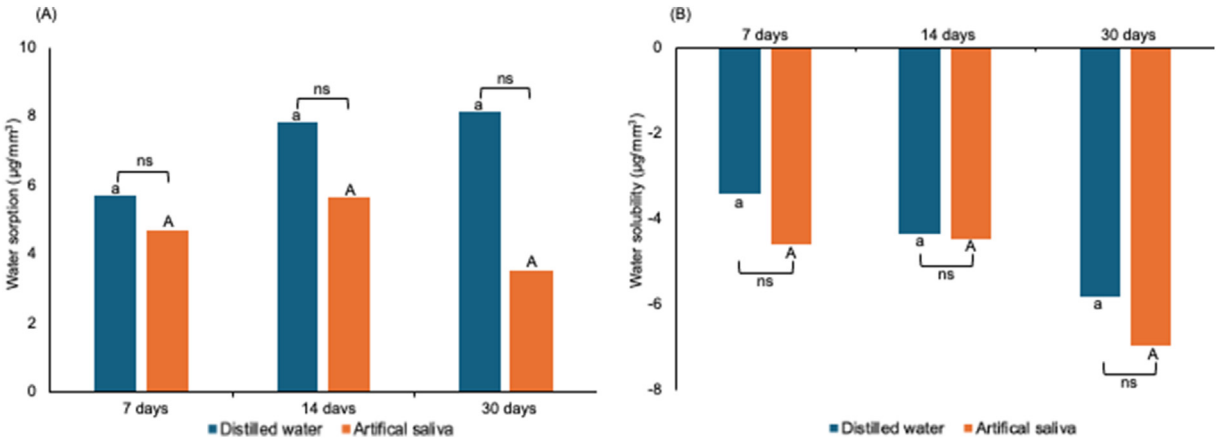

Figure 2 Mean values of (A) water sorption and (B) water solubility of 3D-printed resin specimens immersed in distilled water and artificial saliva for 7, 14, and 30 days. Bars sharing the same letter indicate no significant difference ($P > 0.05$).

Table 2 Measurements of diameter, thickness, and volume of 3D-printed resin over 7, 14, and 30 days.

Solution	Immersion period	Diameter (mm)			Thickness (mm)			Volume (mm^3)		
		T_1	T_2	T_3	T_1	T_2	T_3	T_1	T_2	T_3
Distilled water	7 days	9.78 (0.12)^{a}	9.77 (0.12)^{a}	9.77 (0.11)^{a}	2.35 (0.06)^{d}	2.35 (0.06)^{d}	2.35 (0.06)^{d}	176.39 (5.94)^{g}	176.33 (5.92)^{g}	175.97 (5.47)^{g}
	14 days	9.67 (0.16)^{b}	9.70 (0.15)^{b}	9.70 (0.16)^{b}	2.42 (0.10)^{e}	2.43 (0.09)^{e}	2.42 (0.09)^{e}	178.77 (11.77)^{h}	179.43 (11.32)^{h}	179.43 (11.32)^{h}
	30 days	9.78 (0.19)^{c}	9.78 (0.18)^{c}	9.77 (0.18)^{c}	2.29 (0.08)^{f}	2.28 (0.08)^{f}	2.28 (0.09)^{f}	171.89 (11.02)^{i}	171.15 (12.47)^{i}	171.09 (11.60)^{i}
Artificial saliva	7 days	9.76 (0.24)^{A}	9.77 (0.24)^{A}	9.77 (0.24)^{A}	2.35 (0.10)^{D}	2.36 (0.11)^{D}	2.35 (0.10)^{D}	176.31 (15.67)^{G}	176.84 (16.22)^{G}	176.38 (15.89)^{G}
	14 days	9.83 (0.14)^{B}	9.82 (0.14)^{B}	9.82 (0.14)^{B}	2.35 (0.12)^{E}	2.35 (0.09)^{E}	2.34 (0.09)^{E}	178.04 (10.85)^{H}	177.29 (9.19)^{H}	176.99 (8.93)^{H}
	30 days	9.69 (0.16)^{C}	9.73 (0.15)^{C}	9.74 (0.16)^{C}	2.30 (0.07)^{F}	2.30 (0.06)^{F}	2.30 (0.05)^{F}	170.02 (7.81)^{I}	170.80 (6.51)^{I}	171.13 (7.39)^{I}

T_1 denotes initial measurements before submersion, T_2 after submersion, and T_3 after drying. Values are presented as the mean (standard deviation, SD). Means (SD) followed by the same superscript letter indicate no significant difference ($P > 0.05$).

Fig. 4 illustrates the maximum bending force and deflection distance of 3DR specimens compared to the MSW. The maximum bending force of the MSW was 4.77 ± 0.05 N. Among 3DR specimens, R1.5 (6.57 ± 0.98 N) and H1 (3.89 ± 0.81 N) exhibited no statistically significant difference compared to the MSW. In contrast, the maximum bending forces of R2 (17.94 ± 2.99 N), H1.5 (12.14 ± 2.94 N), and H2.0 (34.90 ± 7.97 N) were significantly higher than that of the MSW, exceeding the requirements for an FLR and potentially compromising patient comfort due to their larger dimensions. Regarding deflection distances, the MSW did not break even at a deflection of 2.0 mm, whereas all 3DR specimens fractured before reaching this limit, showing a significant difference compared to the MSW. Among 3DR specimens, H1 exhibited flexibility characteristics closest to the MSW and deflected significantly farther than the other 3DR samples.

Discussion

FLRs are widely used to maintain orthodontic alignment, but unwanted tooth movements can occur due to non-passive bonding, wire displacement due to external forces such as biting and occlusal stress, and material-related factors such as an untwisting of spiral wires. This phenomenon, known as wire syndrome, is best prevented with a well-fitting passive retainer.[28] In this study, we evaluated 3DR as an alternative to conventional MSW for FLRs.

W_{sp} and W_{sl} significantly influence the mechanical properties, dimensional consistency, and chemical release.[29] AS was used alongside DW to better simulate the oral environment.[30] Furthermore, BZ 109 was chosen because it is specifically designed to test dental products for colorfastness and biodegradability, which closely aligns with the objectives of our study. For the success of an FLR, it is crucial that the material maintains its physical properties, structural stability, and biocompatibility over time. W_{sp} values are typically lower in AS because its ionic content reduces osmotic pressure differences, leading to lower water uptake.[31] Negative solubility values likely indicate incomplete dehydration of the materials rather than true insolubility.[32] Furthermore, strong negative solubility values suggest that components of AS are preferentially adsorbed onto the resin surface,[33] which aligns with the current findings. Dimensional stability was confirmed as the

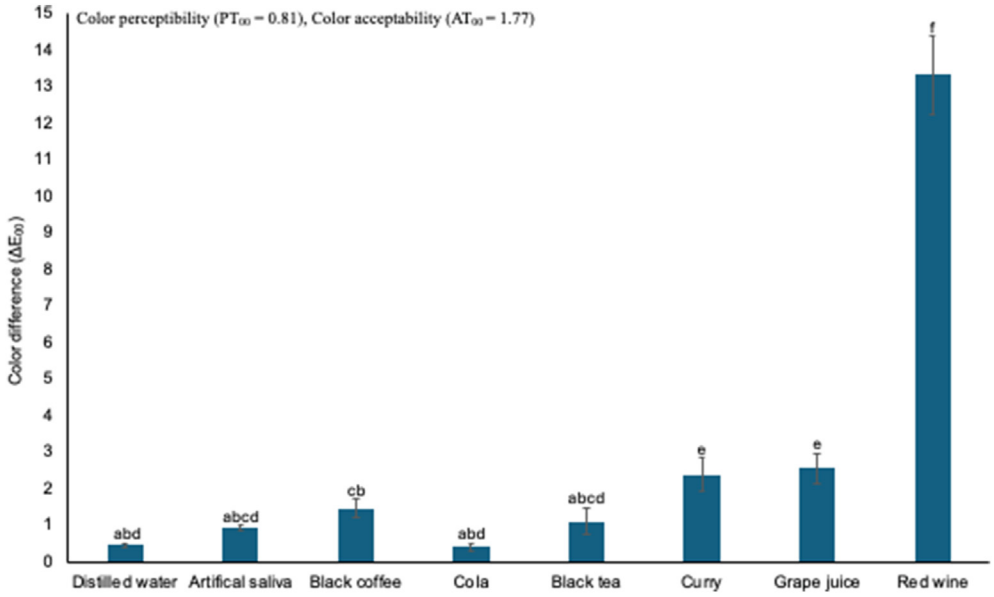

Figure 3 Mean color difference values of 3D-printed resin specimens after immersion in different solutions for 7 days. Bars sharing the same letter indicate no significant difference ($P > 0.05$).

Table 3 Flexural strength of 3D-printed resin specimens with round (R) and hemi-elliptical (H) cross-sections.

Specimens	Flexural strength (MPa)	Significance
R1.5	25.33 ± 3.33	H1.0, H1.5, H2.0
R2.0	22.92 ± 3.26	H1.0, H1.5, H2.0
H1.0	218.47 ± 57.54	R1.5, R2.0, H1.5, H2.0
H1.5	152.43 ± 57.54	R1.5, R2.0, H1.0
H2.0	150.91 ± 57.54	R1.5, R2.0, H1.0

The abbreviations of groups' names are specified in Table 1. Values are shown as the mean ± standard deviation. Specimens listed in the significance column indicate a statistically significant difference ($P < 0.05$) compared to the corresponding specimen in the first column. Flexural strength was measured using a three-point bending test.

diameter, thickness, and volume showed no notable changes before and after immersion or drying. All samples met ISO 4049 standards, indicating good structural stability, resistance to degradation, and compliance with intraoral requirements.[20]

A digital light processing (DLP) 3D printer offers exceptional resolution and rapid printing capabilities but is prone to discoloration.[21] The study ranked staining potential as RW > GJ > CR > BC > BT > AS > DW > cola. RW caused the greatest discoloration, likely due to alcoholic softening of the resin matrix. GJ also caused significant staining, consistent with a previous article, as it contains natural pigments that are absorbed into the resin.[34] CR ranking lower than expected based on previous studies was possibly due to variations in temperature and ingredients.[35] All of the above three solutions resulted in color changes exceeding the limit of acceptability. BC stained more than BT, although the difference was not statistically significant. The staining potential was due to yellow staining molecules in coffee and tannic acid and pigments in tea.[36] Interestingly, AS showed greater staining than cola and DW, which correlated with its adhesion properties.[33,37] Cola demonstrated minimal staining due to its low concentration of yellow colorants with low polarity, despite its acidic pH.[36] As this 3DR is not fully color-resistant, patients should maintain good oral hygiene since FLRs are placed at the back of the anterior teeth. While acidic pH can soften surfaces and increase pigment deposition,[38] RW caused more staining than cola despite having a higher pH. Similarly, BC and CR, despite having a higher pH than cola, resulted in significant discoloration. This suggests that factors such as manufacturing methods, composition, pigment content, and polymer affinity influence ΔE_{00} values more than pH.[21]

The TPBT evaluated flexural strength based on dimensions and the cross-sectional shape, using conventional MSW as a control for the 3DR FLR design. Dimensions were determined according to technician recommendations and typical maxillary and mandibular tooth sizes.[39] Flexural strength for a round cross-section was calculated using a standard equation, while for a hemi-elliptical cross-section, geometric parameters were substituted into the circular equation.[26] Notably, the hemi-elliptical wire demonstrated superior stress resistance compared to the round wire, aligning with previous studies that highlighted its more-favorable stress distribution.[14,19] Flexibility is crucial for FLRs to support physiological tooth movement, preserving periodontal health and minimizing bonding failure.[1] The load-deflection analysis showed that R1.5, R2.0, H1.5, and H2.0 exhibited brittle failure, whereas H1 demonstrated greater flexibility with a gradual load-deflection curve and higher deflection capacity before failure. Sifakakis et al.[40] reported that mandibular incisors exhibited 0.06 mm of anteroposterior mobility at 1.5 N. The control MSW required 0.57 ± 0.09 N for this movement, while H1 required 0.6 ± 0.15 N, confirming its ability to

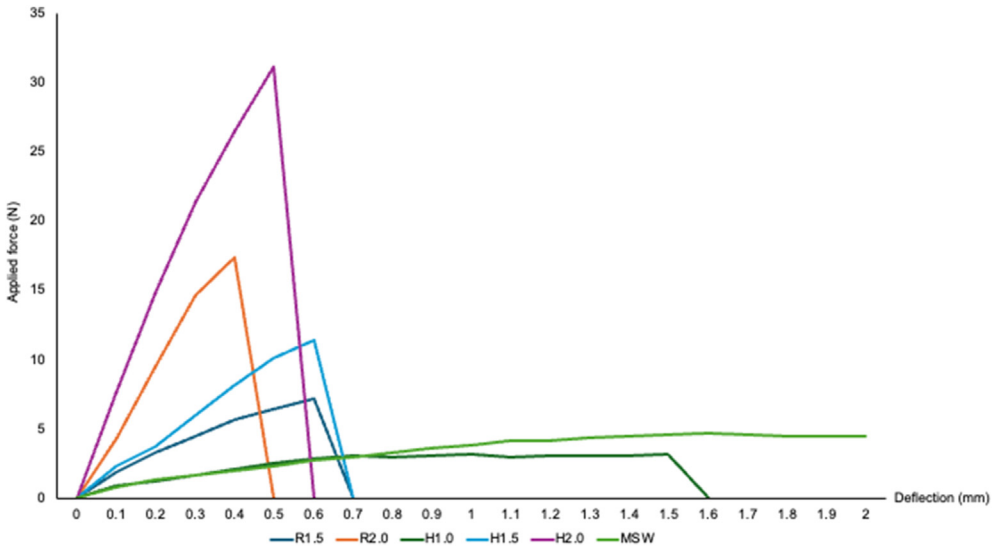

Figure 4 Load-deflection curves of 3D-printed resin (3DR) specimens and multistrand stainless steel wire (MSW). The abbreviations of groups' names are specified in Table 1.

allow physiological tooth movement. MSW, although more flexible, displaced up to 2.0 mm without breaking, potentially leading to stress accumulation and unintended tooth movement.[11,28] In contrast, H1 fractured after 1.5 mm of deflection, serving as an early warning for FLR issues, similar to debonding in a canine-to-canine retainer,[11] prompting timely dental visits.

This study has limitations: water sorption and solubility tests were conducted for 1 month, despite retainers being placed intraorally for years. Additionally, staining tests were performed only at room temperature, omitting temperature variations and post-brushing color restoration. Moreover, BZ 109 does not fully replicate the dynamic nature of natural saliva, some deviations in the results may occur. Further experiments must account for factors such as dynamic pH fluctuations, proteins content and microbial activity to more accurately simulate oral conditions. Additionally, specimens were not printed in a circular form matching the dental arch. Future studies should incorporate vertical biting force assessments and shear bonding tests using arch-shaped specimens. Additionally, aging procedures such as thermocycling should be implemented to better simulate long-term clinical conditions.

In conclusion, 3DR demonstrated excellent W_{sp} and W_{sl} values which were within ISO 4049 standards, ensuring structural stability for intraoral use. While RW, GJ, and CR caused significant staining, proper oral hygiene can help minimize discoloration risks. TPBT identified the optimal FLR design as a hemi-elliptical cross-section (1.0 mm thick and 2.0 mm wide), offering sufficient flexibility for physiological tooth movement while serving as an early failure indicator, preventing unwanted tooth movement. Within the limitation of *in vitro* study, 3DR shows potential as an FLR, providing long-term stability, moderate stainability, and performance comparable to MSW. Further studies including bonding strength test, biofilm formation test, and clinical trials, are needed to assess the efficacy, safety and practical suitability of 3DR as a FLR.

Declaration of competing interests

The authors have no conflicts of interest relevant to this article.

Acknowledgements

The study was supported by National Science and Technology Council of Taiwan [grant number 112-2314-B-038-118-MY2]. The authors thank Mr. Po-En Chuang and Mr. Cheng-Cho Chuang (Evolution Dental Laboratory, Taipei, Taiwan) for technical assistance with manufacturing the specimens.

References

1. Littlewood SJ, Dalci O, Dolce C, Holliday LS, Naraghi S. Orthodontic retention: what's on the horizon? *Br Dent J* 2021; 230:760—4.
2. Al-Moghrabi D, Salazar FC, Pandis N, Fleming PS. Compliance with removable orthodontic appliances and adjuncts: a systematic review and meta-analysis. *Am J Orthod Dentofacial Orthop* 2017;152:17—32.
3. Al-Moghrabi D, Johal A, O'Rourke N, et al. Effects of fixed vs removable orthodontic retainers on stability and periodontal health: 4-year follow-up of a randomized controlled trial. *Am J Orthod Dentofacial Orthop* 2018;154:167—174 e1.
4. Knierim RW. Invisible lower cuspid to cuspid retainer. *Angle Orthod* 1973;43:218—20.
5. Karaman AI, Kir N, Belli S. Four applications of reinforced polyethylene fiber material in orthodontic practice. *Am J Orthod Dentofacial Orthop* 2002;121:650—4.
6. Zachrisson BU. Multistranded wire bonded retainers: from start to success. *Am J Orthod Dentofacial Orthop* 2015;148:724—7.
7. Jahanbin A, Shahabi M, Ahrari F, et al. Evaluation of the cytotoxicity of fiber reinforced composite bonded retainers and flexible spiral wires retainers in simulated high and low cariogenic environments. *J Orthod Sci* 2015;4:13—8.

8. Roser C, Hilgenfeld T, Sen S, et al. Evaluation of magnetic resonance imaging artifacts caused by fixed orthodontic CAD/CAM retainers-an in vitro study. *Clin Oral Invest* 2021;25: 1423—31.
9. ElNaghy R, El-Aassar YM, Hasanin M. Fiber reinforced composite retainers may be as effective as multistranded stainless-steel wires in failure rates and minimal adverse effect, but superior in terms of relapse and patient satisfaction. *J Evid Base Dent Pract* 2023;23:1—3.
10. Scribante A, Sfondrini MF, Broggini S, D'Allocco M, Gandini P. Efficacy of esthetic retainers: clinical comparison between multistranded wires and direct-bond glass fiber-reinforced composite splints. *Int J Dent* 2011:1—5.
11. Shaughnessy TG, Proffit WR, Samara SA. Inadvertent tooth movement with fixed lingual retainers. *Am J Orthod Dentofacial Orthop* 2016;149:277—86.
12. Singh P. Canine avulsion: an extreme complication of a fixed mandibular lingual retainer. *Am J Orthod Dentofacial Orthop* 2021;160:473—7.
13. Stout MM, Cook BK, Arola DD, Fong H, Raigrodski AJ, Bollen AM. Assessing the feasibility of yttria-stabilized zirconia in novel designs as mandibular anterior fixed lingual retention after orthodontic treatment. *Am J Orthod Dentofacial Orthop* 2017; 151:63—73.
14. Win PP, Chen DD, Sainbayar B, Peng TY, Cheng JH. Assessment of mechanical characteristics of polyetheretherketone as orthodontic fixed lingual retainers. *J Dent Sci* 2023;18:1804—11.
15. Alabbadi AA, Abdalla EM, Hanafy SA, Yousry TN. A comparative study of CAD/CAM fabricated polyether ether ketone and fiber-glass reinforcement composites versus metal lingual retainers under vertical load (an in vitro study). *BMC Oral Health* 2023; 23:583.
16. Sidhom M, Zaghloul H, Mosleh IE, Eldwakhly E. Effect of different CAD/CAM milling and 3D printing digital fabrication techniques on the accuracy of PMMA working models and vertical marginal fit of PMMA provisional dental prosthesis: an in vitro study. *Polymers* 2022;14:1285.
17. Ellakany P, Fouda SM, Mahrous AA, AlGhamdi MA, Aly NM. Influence of CAD/CAM milling and 3D-printing fabrication methods on the mechanical properties of 3-unit interim fixed dental prosthesis after thermo-mechanical aging process. *Polymers* 2022;14:4103.
18. Firlej M, Zaborowicz K, Zaborowicz M, et al. Mechanical properties of 3D printed orthodontic retainers. *Int J Environ Res Publ Health* 2022;19:5775.
19. Alnuaimy NS, Alhuwaizi AF. A novel 3-dimensional printed nanoceramic hybrid resin fixed lingual retainer: characterization and mechanical tests. *Int J Dent* 2024:1—14.
20. International Organization for Standardization. *ISO 4049:2019. Dentistry — polymer-based restorative materials*. Geneva: ISO, 2019.
21. Lee SY, Lim JH, Kim D, Lee DH, Kim SG, Kim JE. Evaluation of the color stability of 3D printed resin according to the oxygen inhibition effect and temperature difference in the post-polymerization process. *J Mech Behav Biomed Mater* 2022; 136:1—11.
22. Lee WF, Takahashi H, Huang SY, Zhang JZ, Teng NC, Peng PW. Effects of at-home and in-office bleaching agents on the color recovery of esthetic CAD-CAM restorations after red wine immersion. *Polymers* 2022;14:3891.
23. Luo MR, Cui G, Rigg B. The development of the CIE 2000 colour-difference formula: CIEDE2000. *Color Res Appl* 2001;26: 340—50.
24. Paravina RD, Ghinea R, Herrera LJ, et al. Color difference thresholds in dentistry. *J Esthetic Restor Dent* 2015;27(Suppl 1):S1—9.
25. International Organization for Standardization. *ISO 15841: 2014. Dentistry — Wires for use in orthodontics*. Geneva: ISO, 2014.
26. Alander P, Lassila LV, Vallittu PK. The span length and cross-sectional design affect values of strength. *Dent Mater* 2005; 21:347—53.
27. Perez MM, Della Bona A, Carrillo-Perez F, Dudea D, Pecho OE, Herrera LJ. Does background color influence visual thresholds? *J Dent* 2020;102:1—6.
28. Charavet C, Vives F, Aroca S, Dridi SM. "Wire syndrome" following bonded orthodontic retainers: a systematic review of the literature. *Healthcare (Basel)* 2022;10:379.
29. Muller JA, Rohr N, Fischer J. Evaluation of ISO 4049: water sorption and water solubility of resin cements. *Eur J Oral Sci* 2017;125:141—50.
30. Schipper RG, Silletti E, Vingerhoeds MH. Saliva as research material: biochemical, physicochemical, and practical aspects. *Arch Oral Biol* 2007;52:1114—35.
31. Saini R, Kotian R, Madhyastha P, Srikant N. Comparative study of sorption and solubility of heat-cure and self-cure acrylic resins in different solutions. *Indian J Dent Res* 2016;27:288—94.
32. Albilali AT, Baras BH, Aldosari MA. Evaluation of water sorption and solubility and FTIR spectroscopy of thermoplastic orthodontic retainer materials subjected to thermoforming and thermocycling. *Appl Sci (Basel)* 2023;13:5165.
33. Alshali RZ, Salim NA, Satterthwaite JD, Silikas N. Long-term sorption and solubility of bulk-fill and conventional resin-composites in water and artificial saliva. *J Dent* 2015;43: 1511—8.
34. Silva HA, Arossi GA, Damo DM, Tovo MF. Effect of grape derived beverages in colour stability of composite resin submitted to different finishing and polishing methods. *Pesqui Bras Odontopediatria Clin Integr* 2017;17:1—10.
35. Huang W, Ren L, Cheng Y, et al. Evaluation of the color stability, water sorption, and solubility of current resin composites. *Materials* 2022;15:6710.
36. Arocha MA, Mayoral JR, Lefever D, Mercade M, Basilio J, Roig M. Color stability of siloranes versus methacrylate-based composites after immersion in staining solutions. *Clin Oral Invest* 2013;17:1481—7.
37. Rai AV, Naik BD. The effect of saliva substitute on the color stability of three different nanocomposite restorative materials after 1 month: an in vitro study. *J Conserv Dent* 2021;24:50—6.
38. Bagheri R, Burrow MF, Tyas M. Influence of food-simulating solutions and surface finish on susceptibility to staining of aesthetic restorative materials. *J Dent* 2005;33:389—98.
39. Choi SH, Kim JS, Kim CS, Yu HS, Hwang CJ. Cone-beam computed tomography for the assessment of root-crown ratios of the maxillary and mandibular incisors in a Korean population. *Korean J Orthod* 2017;47:39—49.
40. Sifakakis I, Pandis N, Eliades T, Makou M, Katsaros C, Bourauel C. In-vitro assessment of the forces generated by lingual fixed retainers. *Am J Orthod Dentofacial Orthop* 2011; 139:44—8.